Werk

Jahr: 1978
Kollektion: fid.geo
Signatur: 8 Z NAT 2148:45
Digitalisiert: Niedersächsische Staats- und Universitätsbibliothek Göttingen
Werk Id: PPN1015067948_0045
PURL: http://resolver.sub.uni-goettingen.de/purl?PPN1015067948_0045

LOG Id: LOG_0065
LOG Titel: A theoretical investigation of the dipole- and unipole-resistivity methods for geoelectrical prospecting in Marine areas
LOG Typ: article

Übergeordnetes Werk

Werk Id: PPN1015067948
PURL: http://resolver.sub.uni-goettingen.de/purl?PPN1015067948
OPAC: http://opac.sub.uni-goettingen.de/DB=1/PPN?PPN=1015067948

Contact

Niedersächsische Staats- und Universitätsbibliothek Göttingen
Georg-August-Universität Göttingen
Platz der Göttinger Sieben 1
37073 Göttingen
Germany
Email: gdz@sub.uni-goettingen.de

J. Geophys. 45, 409–416, 1979

Journal of Geophysics

A Theoretical Investigation of the Dipole- and Unipole-Resistivity Methods for Geoelectrical Prospecting in Marine Areas

J. Sebulke and W. Hildebrandt

Institut für Angewandte Geophysik, Petrologie und Lagerstättenforschung
der Technischen Universität Berlin, Straße des 17. Juni 135, EB 15, 1000 Berlin 12

Abstract. The apparent resistivity of a dipole-dipole and a unipole-configuration has been calculated based on the potential of a buried electrode. The model calculations indicate that the thickness of seafloor sediments can be determined with good accuracy; however, the results cannot be expected better than by application of the two-electrode configurations, which were described in previous papers (Sebulke, 1973; 1978).

Key words: Marine geoelectrical sounding – Dipole- and unipole-resistivity measurements – Computed apparent resistivity.

1. Introduction

Within the last seven years investigations of the resistivity method for use in marine areas have been carried out at the department of Applied Geophysics (Institut of Applied Geophysics, Petrology, Economic and Mining Geology) at the Technical University of Berlin. In different papers (Sebulke, 1973; Bischoff and Sebulke, 1976) special configurations for marine resistivity measurements have been suggested. Results of field measurements with different two-electrode configurations have been published (e.g., Bischoff, 1978).

The present article (being based on a diploma thesis by Hildebrandt, 1976) discusses the possibility of using dipole-dipole and unipole measuring arrays in marine resistivity prospecting. The aim of the theoretical investigations is to find out, if the two examined configurations have any advantages in comparison to the two-electrode configurations.

2. Theoretical Foundation

The potential of a buried physical electrical dipole is deducible when using the potential of a buried electrical point-source. The considered model is the horizontally stratified three-layered-earth with homogenous and isotropic re-

0340-062X/79/0045/0409/$01.60

sistivities. The potential of a buried electrical point source is well known (Therekin, 1962; Alfano, 1962; Merkel, 1971). It can be calculated by the complementary solution of the Laplace's equation in cylindrical coordinates (Stefanesco et al., 1930) and by the application of the boundary conditions of the stationary electrical field applied to the generally formulated potentials.

The following form of the potentials was introduced by Sebulke (1973; 1978).

$$V_p = V(r, z)$$
$$= q_j \left(A_j + C_j \int_0^\infty \frac{\sum_i g_i e^{-2\lambda b_i}}{1 - k_1 e^{-2\lambda h_1} - k_2 e^{-2\lambda h_2} + k_1 k_2 e^{-2\lambda(h_2 - h_1)}} J_0(\lambda r)\, d\lambda \right). \quad (1)$$

where

j = index of the layer where the point source is situated

$$q_j = \frac{\rho_j \cdot I}{4\pi}. \quad (2)$$

A_j = term, which describes the primary potential

C_j = factor, which depends on the layer where the source and testpoint are placed

g_i = coefficients of numerator polynomal of the Kernel function, they depend on the position of current and potential electrodes in the different layers

$J_0(\lambda r)$ = Bessel function of zero order

λ = constant from the separation of the Laplace's equation

h_n = depth of the lower boundary of layer n

r = horizontal distance between the point source and the test point

$k_n = \frac{\rho_{n+1} - \rho_n}{\rho_{n+1} + \rho_n}$ resistivity contrast.

The fully written formulas will be found in the appendix.

The improper integral in Eq. (1) can be easy transformed into infinite convergent series by means of the Weber-Lipschitz formula. The potential of an inclined dipole (Fig. 1) can be derived from the point electrode potential as follows:

$$V_D = -\left(\frac{\partial V_p}{\partial r} L \cos\alpha + \frac{\partial V_p}{\partial z} L \sin\alpha \right) = -\operatorname{grad} V_p \cdot \vec{L} \quad (3)$$

where $E_1 E_2 = L$ = length of the inclined current dipole and α = inclination of the current dipole.

The test point is situated in a vertical plane across the physical current dipole.

For a dipole-dipole configuration as presented in Fig. 1 the apparent resistivity is (horizontal measuring dipol):

$$\rho_s = K \left(-\frac{\partial V_D}{\partial r} \right) \frac{1}{I} \quad (4)$$

with

K = configuration factor

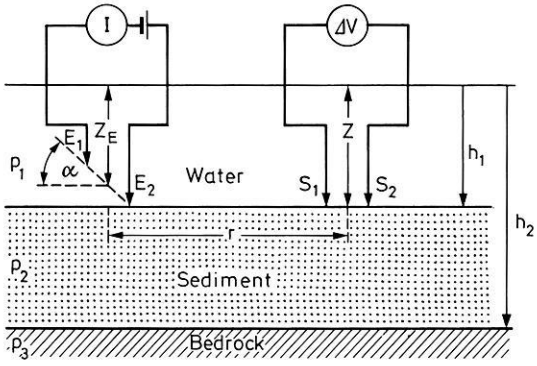

Fig. 1. The dipole-dipole configuration for use in marine resistivity sounding and the assumed model of the ground (Both dipoles in a joint vertical plane). Z_E: depth of the current dipole; Z: depth of the measuring dipole in the halfspace; E_1, E_2: electrodes of the current dipole; S_1, S_2: electrodes of the potential dipole

and

$S_1 S_2 = 1 =$ length of the measuring dipole.

The condition must hold, that the length of the both dipoles is very small in comparision to the distance r. For the special case in which the current electrodes and the two potential probes are placed either on the bottom of the sea or both in the sediment we can use for further computations the potential of a point electrode and a test point located in layer 2 (A 4). We get the following expression for the apparent resistivity:

$$\rho_s = \rho_2 K_D^* \left[\frac{1}{r} \cos\alpha \int_0^\infty (e^{-\lambda(z_E - z)} + \Theta_2(\lambda) e^{-\lambda z} + \Psi_2(\lambda) e^{+\lambda z}) \lambda J_1(\lambda r) d\lambda \right.$$
$$- \cos\alpha \int_0^\infty (e^{-\lambda(z_E - z)} + \Theta_2(\lambda) e^{-\lambda z} + \Psi_2(\lambda) e^{+\lambda z}) \lambda^2 J_0(\lambda r) d\lambda$$
$$\left. - \sin\alpha \int_0^\infty (e^{-\lambda(z_E - z)} - \Theta_2(\lambda) e^{-\lambda z} + \Psi_2(\lambda) e^{+\lambda z}) \lambda^2 J_1(\lambda r) d\lambda \right] \tag{5}$$

with

$$K_D^* = \frac{[r^2 + (z_E - z)^2]^{5/2} [r^2 + (z_E + z)^2]^{5/2}}{3r[r^2 + (z_E + z)^2]^{5/2} [r \cdot \cos\alpha - (z_E - z)\sin\alpha] - [r^2 + (z_E - z)^2]}$$
$$\times [r^2 + (z_E + z)^2]^{5/2} \cos\alpha + 3r[r^2 + (z_E - z)^2]^{5/2} [r\cos\alpha - (z_E + z)\sin\alpha]$$
$$- [r^2 + (z_E - z)^2]^{5/2} [r^2 + (z_E + z)^2] \cos\alpha \tag{6}$$

and

$$\Theta_2(\lambda) = \frac{e^{-\lambda z_E} - k_1 e^{-\lambda(z_E - 2h_1)} + k_2 e^{-\lambda(2h_2 - z_E)} - k_1 k_2 e^{-\lambda(2h_2 - 2h_1 - z_E)}}{1 - k_1 e^{-2\lambda h_1} - k_2 e^{-2\lambda h_2} + k_1 k_2 e^{-2\lambda(h_2 - h_1)}} \tag{7}$$

$$\Psi_2(\lambda) = \frac{k_2 [e^{-\lambda(2h_2 - z_E)} + e^{-\lambda(2h_2 + z_E)}] - k_1 k_2 [e^{-\lambda(2h_2 + 2h_1 - z_E)} + e^{-\lambda(2h_2 - 2h_1 + z_E)}]}{1 - k_1 e^{-2\lambda h_1} - k_2 e^{-2\lambda h_2} + k_1 k_2 e^{-2\lambda(h_2 - h_1)}}. \tag{8}$$

$\Theta_2(\lambda)$, $\Psi_2(\lambda)$ = Kernel functions for the three layer case

$J_1(\lambda)$ = Bessel function of the first order.

The symbols of the parameters are the same as previously used by Flathe (1955).

3. Results of the Calculations for Dipole-Measurements

A large number of model graphs obtained with a FORTRAN IV computer program (Hildebrandt, 1976) were examined upon the possibility to determine the sediment's thickness. Some of them will be presented here.

Figure 2a and b show the results of model calculations for two different inclinations of the current dipole. The resistivity ratios are based on results from field measurements in the Mediterranean (Bischoff and Sebulke, 1976).

The graphs show that different thicknesses of the sediment can be resolved with a good accuracy but there is no improvement upon the results of the formerly published two-electrode configurations. Figure 3 shows calculations for the symmetrical two-electrode configuration derived for the same model as before.

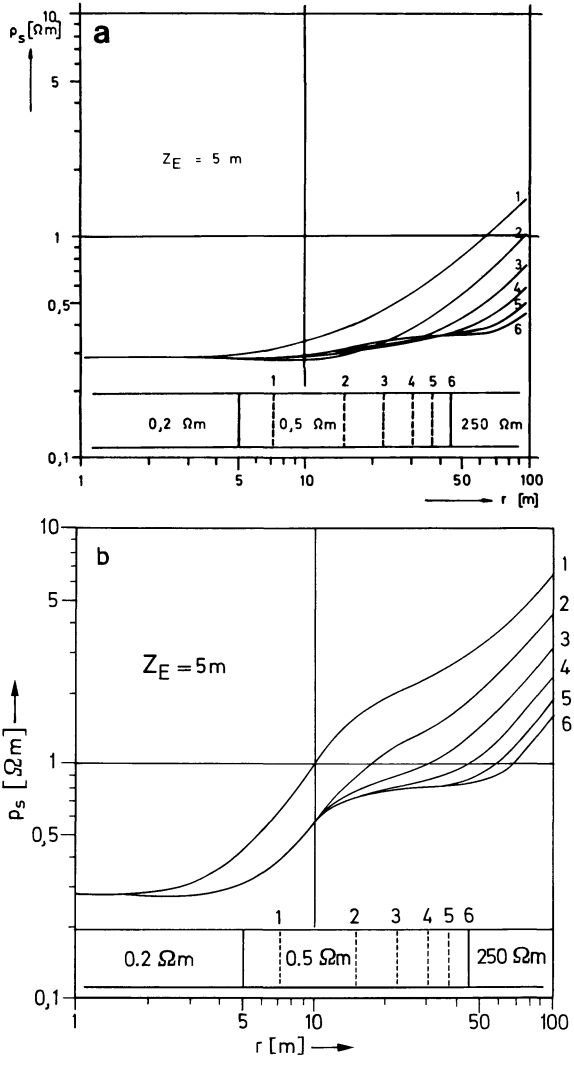

Fig. 2a and b. Computed apparent resistivity for the dipole-dipole configuration for various thicknesses of the sediment layer
a Inclination of the current-dipole $\alpha = 0°$
b Inclination of the current-dipole $\alpha = 120°$
(current- and potential-electrodes on the seafloor, $Z_E = Z = h_1 = 5$ m, the resistivities and thicknesses of the layers are demonstrated in the logarithmic sectional drawing)

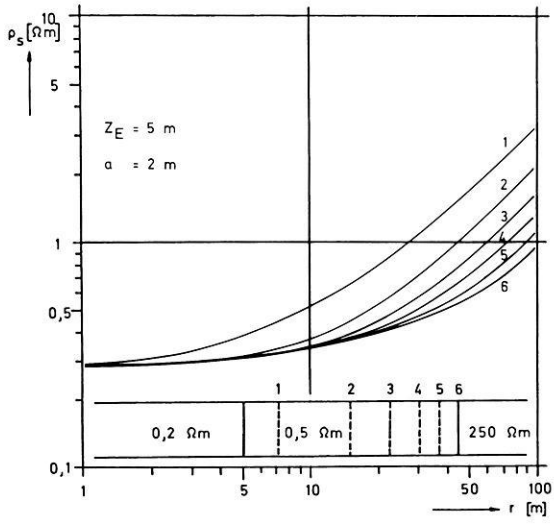

Fig. 3. Computed apparent resistivity for the symmetrical two-electrode configuration for various thicknesses of the sediment layer (current- and potential-electrodes on the seafloor, $Z_E = Z = h_1 = 5$ m)

4. Results for the Unipole-Configuration

The unipole-configuration is shown in Fig. 4. Two electrodes with the same polarity generate the electrical field. The potential difference is measured with one probe against a physical infinite located point.

The corresponding formula for the apparent resistivity of this configuration can be deduced from the point-electrode-potential (1). If the current-electrodes and the potential-electrode are situated all in the first sediment layer the apparent resistivity will be calculated using formula (A 4).

$$\rho_s = \rho_2 K_u^* \int_0^\infty [e^{\pm\lambda(z_E - z)} + \Theta_2(\lambda)\, e^{-\lambda z} + \Psi_2(\lambda)\, e^{+\lambda z}]\, [J_0(\lambda r) + J_0(\lambda 2r)]\, d\lambda. \qquad (9)$$

The reduced configuration factor K_u^* depends only on the geometrical position of the electrodes in this three-point-configuration and is defined as:

$$K_u^* = \frac{1}{[r^2 + (z_E - z)^2]^{-1/2} + [r^2 + (z_E + z)^2]^{-1/2} + [4r^2 + (z_E - z)^2]^{-1/2} + [4r^2 + (z_E + z)^2]^{-1/2}}$$

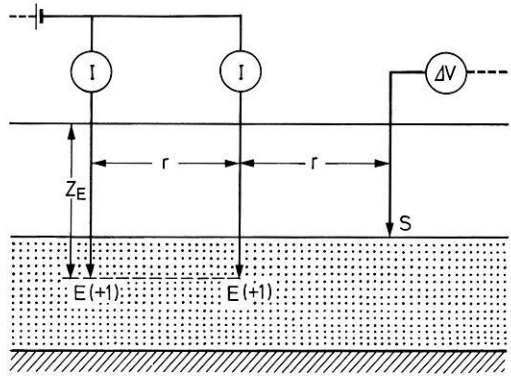

Fig. 4. The unipole-configuration for use in marine resistivity sounding

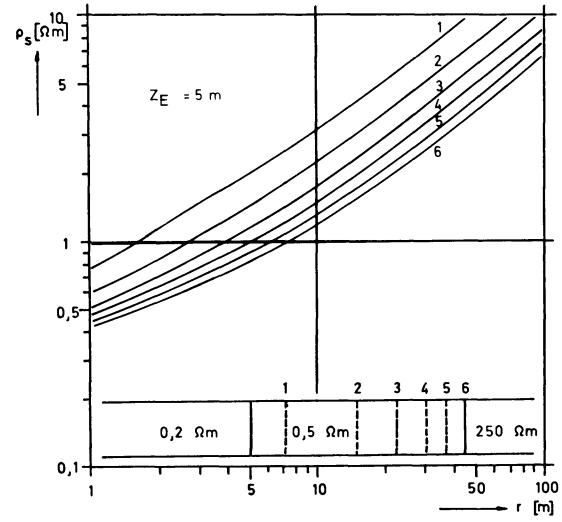

Fig. 5. Computed apparent resistivity for the unipole configuration for various thicknesses of the sediment layer (current- and potential-electrodes on the seafloor, $Z_E = Z = h_1 = 5$ m)

$\Theta_2(\lambda)$ and $\Psi_2(\lambda)$ are the same Kernel functions for the three-layer-case as given before (7), (8).

One example of calculated apparent resistivities for the described unipol configuration is shown in Fig. 5. The model is the same as that of the dipole-computation in Fig. 2. It is obvious that the differences between the curves for various thicknesses of the second layer (sediment) are sufficient to determine that thickness with a good accuracy (until a thickness of about 30 m); however, the resolving power is not better than that for the two-electrode configuration (s. Fig. 3) and the dipole-dipole configuration (s. Fig. 2).

5. Conclusion

Several model calculations have been done to compute the apparent resistivity of the here described dipole-dipole configuration and the unipole array. Some of the results are presented in this paper. It may be concluded that both examined configurations could be used for marine geoelectrical prospecting.

Practical measurements with different two-electrode configurations have been carried out in the Mediterranean and in the North Sea. A digital measuring system was used. The current electrodes and the electrodes for the determination of the potential differences are connected at a towed multiple conductor cable, which is layed out on the seafloor. The potential electrodes are scanned by an automatic scanner and the data are recorded computer compatible on a digital cassette recorder. The potential differences measured with such an array are very small. Using a dipole-dipole configuration the potential differences will become smaller than the one hundredth part of that obtainable with a two-electrode configuration. Using a unipole configuration it is necessary to bring a second potential electrode to a physical infinit point. Because the dipole-dipole and unipole configurations cannot be expected better results in

resolving the thickness of the sediment layers than the two-electrode configurations, which moreover have some advantages in measuring techniques, practical measurements with the both presented configurations have not been excuted and have not been projected in the future.

Acknowledgement. The valuable suggestions of three unknown referees are gratefully acknowledged.

Appendix

Potentials of buried point sources and test points in different layers:

1. Potential-Electrode in Layer 1

1.1. Current-Electrode in Layer 1:

$$V(r,z)=q_1\left[\frac{1}{(r^2+(z-z_E)^2)^{1/2}}+\frac{1}{(r^2+(z+z_E)^2)^{1/2}}\right.$$
$$+\int_0^\infty \frac{k_1(e^{-\lambda(2h_1-z_E)}+e^{-\lambda(2h_1+z_E)})+k_2(e^{-\lambda(2h_2-z_E)}+e^{-\lambda(2h_2+z_E)})}{1-k_1e^{-2\lambda h_1}-k_2e^{-2\lambda h_2}+k_1k_2e^{-2\lambda(h_2-h_1)}}$$
$$\left.\cdot(e^{-\lambda z}+e^{\lambda z})\,J_0(\lambda r)\,d\lambda\right]. \tag{A1}$$

1.2. Current Electrode in Layer 2:

$$V(r,z)=q_2(1-k_1)\int_0^\infty \frac{(e^{-\lambda z_E}+k_2e^{-\lambda(2h_2-z_E)})(e^{-\lambda z}+e^{\lambda z})}{1-k_1e^{-2\lambda h_1}-k_2e^{-2\lambda h_2}+k_1k_2e^{-2\lambda(h_2-h_1)}}J_0(\lambda r)\,d\lambda. \tag{A2}$$

1.3. Current Electrode in Layer 3:

$$V(r,z)=q_3(1-k_1)(1-k_2)$$
$$\cdot\int_0^\infty \frac{e^{-\lambda z_E}(e^{-\lambda z}+e^{\lambda z})}{1-k_1e^{-2\lambda h_1}-k_2e^{-2\lambda h_2}+k_1k_2e^{-2\lambda(h_2-h_1)}}J_0(\lambda r)\,d\lambda. \tag{A3}$$

2. Potential- and Current-Electrode in Layer 2

$$V(r,z)=q_2\left(\frac{1}{[r^2+(z-z_E)^2]^{1/2}}\right.$$
$$+\int_0^\infty \frac{[e^{-\lambda z_E}-k_1e^{-\lambda(z_E-2h_1)}+k_1e^{-\lambda(2h_2-z_E)}-k_1k_2e^{-\lambda(2h_2-h_1-z_E)}]e^{-\lambda z}}{1-k_1e^{-2\lambda h_1}-k_2e^{-2\lambda h_2}+k_1k_2e^{-2\lambda(h_2-h_1)}}$$
$$\left.+\frac{+[k_2(e^{-(2h_2-z_E)}+e^{-(2h_2+z_E)})-k_1k_2(e^{-(2h_2+2h_1-z_E)}+e^{-\lambda(2h_2-2h_1+z_E)})]e^{+\lambda z}}{}\right)J_0(\lambda r)\,d\lambda). \tag{A4}$$

3. Potential- and Current-Electrode in Layer 3

$$V(r,z)=q_3\left[\frac{1}{[r^2+(z-z_E)^2]^{1/2}}\right.$$
$$\left.+\int_0^\infty \frac{(e^{-\lambda z_E}-k_1e^{-\lambda(z_E-2h_1)}-k_2e^{-\lambda(z_E-2h_2)}+k_1k_2e^{-\lambda(2h_1+z_E-2h_2)})e^{-\lambda z}}{1-k_1e^{-2\lambda h_1}-k_2e^{-2\lambda h_2}+k_1k_2e^{-2\lambda(h_2-h_1)}}J_0(\lambda r)\,d\lambda\right]. \tag{A5}$$

References

Alfano, L.: Geoelectrical prospecting with underground electrodes. Geophys. Prospect. **10**, 290–303, 1962

Bischoff, J.: Die Anwendung geoelektrischer Widerstandsmethoden im marinen Bereich. Dissertationsschrift D 83. Berlin: Technische Universität 1978

Bischoff, J.; Sebulke, J.: Geoelektrische Widerstandsverfahren zur Prospektion im marinen Bereich. Kongreßberichtswerk Bd. 2. Interocean 1976, 1081–1090, 1976

Flathe, H.: A practical method of calculation geoelectrical model graphs for horizontal stratified media. Geophys. Prospect. **3**, 268–294, 1955

Hildebrandt, W.: Modifizierung unterschiedlicher Konfigurationen bekannter Widerstandsverfahren für den Einsatz im marinen Bereich zur Erhöhung der Interpretationsgenauigkeit. Diplomarbeit. Berlin: Technische Universität 1976

Merkel, R.H.: Resistivity analysis for plane-layer-half-space models with buried current sources. Geophys. Prospect. **19**, 626–639, 1971

Sebulke, J.: Entwicklung und Untersuchung einer Widerstandsmethodik zur geoelektrischen Prospektion im marinen Bereich. Dissertationsschrift D83. Berlin: Technische Universität 1973

Sebulke, J.: The theoretical investigation of resistivity methods for geoelectrical prospecting in marine areas. J. Geophys. **44**, 245–255, 1978

Stefanesco, S.; Schlumberger, C.; Schlumberger, M.: Sur la distribution électrique potentielle autour d'une prise de terre ponctuelle dans un terrain á chouches horizontales, homogénes et isotropes. J. Phys. Rad. **1**, 132–140, 1930

Terekhin, E.I.: Theoretical bases of electrical probing with an apparatus immersed in water. In: Applied Geophysics USSR, N. Rast, ed.: pp. 169–195. Oxford: Pergamon Press 1962

Received July 4, 1978; Revised Version May 22, 1979;
Accepted May 25, 1979